



Published in final edited form as:

Small. 2008 June ; 4(6): 721–727. doi:10.1002/sml.200700754.

Adsorption of Essential Micronutrients by Carbon Nanotubes and the Implications for Nanotoxicity Testing**

Dr. Lin Guo,

Division of Engineering, Brown University, Providence, RI 02912 (USA)

Dr. Annette Von Dem Bussche,

Department of Pathology and Laboratory Medicine, Brown University, Providence, RI 02912 (USA)

Michelle Buechner,

Department of Pathology and Laboratory Medicine, Brown University, Providence, RI 02912 (USA)

Aihui Yan,

Department of Chemistry Brown University, Providence, RI 02912 (USA)

Prof. Agnes B. Kane, and

Department of Pathology and Laboratory Medicine, Brown University, Providence, RI 02912 (USA), Fax: (+1) 401-863-9008

Prof. Robert H. Hurt

Division of Engineering, Brown University, Providence, RI 02912 (USA), Fax: (+1) 401-863-9120

Agnes B. Kane: agnes_kane@brown.edu; Robert H. Hurt: robert_hurt@brown.edu

Keywords

amino acids; biological activity; carbon nanotubes; toxicology; vitamins

Nanotoxicology and nanomedicine make extensive use of in vitro cellular assays that were developed prior to the nanotechnology era. The introduction of nanomaterials to these standard assays causes problems that are currently limiting progress in the field.^[1] Nanoparticles are often difficult to disperse;^[2] they can interfere with optical measurements through light absorption, and they can interact with dyes used as molecular probes of cellular integrity.^[3] In some cases the resulting artifacts can lead to gross misinterpretation of effects on cell viability and cytotoxicity.^[4] Because sp²-hybridized carbon materials are near-universal sorbents for organic compounds in aqueous phases, and in light of a recent report of favorable noncovalent interactions between small-aromatic-molecule therapeutic agents and single-walled carbon nanotubes (SWNTs),^[5] we hypothesize that SWNTs will adsorb a wide variety of small organic solutes from biological media, not limited to indicator dyes or their water-insoluble reduction products.

Herein, we use biochemical profiling techniques and UV/visible spectroscopy to show that SWNTs cause dose-dependent adsorption and depletion of over 14 amino acids and vitamins

**Financial support was provided by the National Science Foundation (NIRT Grant 0506661), the NIEHS Superfund Basic Research Program (P42 ESO13660), and EPA STAR Grant RD-83171901-0.

© 2008 Wiley-VCH Verlag GmbH & Co. KGaA, Weinheim

Correspondence to: Agnes B. Kane, agnes_kane@brown.edu; Robert H. Hurt, robert_hurt@brown.edu.

from RPMI cell culture medium. HepG2 cells cultured in these depleted media show significantly reduced viability, which can be largely restored by replenishment of folate. We have thus demonstrated a fundamentally new mechanism through which hydrophobic nanotube formulations influence cell behavior *indirectly*—that is, without physical contact between the nanotubes and cells. This mechanism, based on depletion of essential micronutrients, must be carefully considered when reporting and interpreting in vitro cytotoxicity assays.

Several recent studies have reported artifacts in nanotoxicology assays arising from interactions between nanomaterials and chemical or fluorescent probes. For example, Worle-Knirsch and co-workers reported that the common 3-(4,5-dimethylthiazol-2-yl)-2,5-diphenyltetrazolium bromide (MTT) assay for cell viability gives false indication of cytotoxicity when applied to carbon nanotubes (CNTs).^[6] In this assay, the MTT salt is reduced by mitochondrial dehydrogenases to the water-insoluble MTT formazan, which is then extracted and photometrically quantified at 550 nm as a measure of cell viability. Worle-Knirsch et al. reported that the MTT formazan crystals associate with SWNTs and are not effectively extracted through the standard protocol, thus leading to low optical absorbance (60% of control) and a false indication of low viability or high cytotoxicity.^[6] Casey et al.^[7] recently presented Raman spectroscopic evidence for nanotube interactions with cell culture medium and reported that nanotube–dye interactions make a number of standard assays unsuitable for quantitative assessment of cytotoxicity. They also suggested that these interactions could produce a secondary cytotoxicity through medium alteration.^[7]

The problems are not limited to CNTs, but have also been reported for carbon black used as a negative control in cytotoxicity assays.^[8] Monteiro et al.^[8] used four sources of carbon black as negative control samples in a study of human keratinocyte cytotoxicity. Conflicting results were obtained across all cytotoxicity endpoints due to problems associated with adsorption of viability indicators onto carbon black surfaces. The same group reported that cytokines IL-6, IL-8, IL-10, and TNF- α can also be adsorbed by water-soluble SWNTs at doses from 0.0005 to 0.5 mg mL⁻¹, which may cause underreporting of cytokine release.^[9]

In each of these cases the underlying phenomena involve some interaction between nanomaterials and organic small-molecule solutes in multicomponent biological phases. While there has been great interest in the fundamental interaction of CNTs with biological *macromolecules*,^[10] less attention has been paid to the fundamental interactions of nanotubes with *small* biomolecules in complex physiological fluid phases (for example, see Roman et al.^[11] or Liu et al.^[5]). The objectives of the present study are therefore threefold: 1) to quantify the effect of CNT exposure on a wide range of small-molecule solutes in cell culture medium; 2) to identify the primary *mechanism* of the nanotube–biomolecule interaction; and 3) to characterize the effect of medium depletion on cell viability and its implications for nanotoxicity testing.

Our interest in nanotube–media interactions began during a study of metal catalyst residues in SWNTs^[12] with the observation that small quantities of nanotubes removed the color associated with the pH indicator dye, phenol red, in cell culture medium (also reported by Casey et al.^[13]). Such small-solute interactions can be conveniently studied by incubating purified SWNTs (see Figure 1) in medium and removing them completely by centrifugal ultrafiltration followed by spent medium biochemical analysis, UV/visible adsorption, and exposure to target cells in culture (see Experimental Section). Optical adsorption at 560 nm was used to quantify phenol red removal, which showed 90% depletion of the dye after addition of only 80 μ g mL⁻¹ of SWNTs to RPMI cell culture medium.

The effect on a broad spectrum of amino acids and vitamins is shown by the biochemical profiles in Figures 2 and 3. Some amino acids, including glycine (GLY), threonine (THR), and glutamic acid (GLU), are not significantly affected up to CNT doses of 10 mg mL^{-1} , while others, including tyrosine (TYR), phenylalanine (PHE), and methionine (MET), are affected at 1 mg mL^{-1} and are largely removed at a SWNT dose of 10 mg mL^{-1} . These doses are beyond the range used in most toxicity assays, but may be relevant to some nanomedicine applications in which cells are plated onto CNT scaffolds or nanostructured surfaces. The vitamin behavior is even more variable, and some vitamins are affected at the lower doses typical of toxicity assays, such as folate and riboflavin, which fall below the detection limit after only 0.1 and 0.01 mg mL^{-1} of CNT addition, respectively. The three compounds adsorbed most readily (folate, riboflavin, and thiamine) all contain planar conjugated units, which have a known high affinity for carbon surfaces driven by π - π interactions.^[15] The lower affinity for free amino acids is consistent with their structure, which lacks polyaromaticity and includes zwitterionic backbones at physiological pH values, thus causing end-group hydrophilicity that is an important factor in the solubility and adsorption of these low-molecular-weight biomolecules.

The trends within the amino acid set provide evidence for a physical driving force in the adsorption mechanism (Figure 4). The fractional amount adsorbed ($\Delta C/C_0$), where ΔC is the concentration change in solution upon adsorption and C_0 is the initial concentration, at a given CNT dose (Figure 4) shows a positive correlation with the hydrophobicity index of the side chain as calculated by Black and Mould,^[16] based on the hydrophobic fragmental constant approach of Rekker.^[17] Hydrophobic interactions are typically a significant driving force for the physical adsorption of organic molecules from solution onto carbon surfaces. There are important outliers in Figure 4, however, including leucine (LEU), isoleucine (ILE), and valine (VAL), which show an anomalous low adsorption for their hydrophobicity, and arginine (ARG) and histidine (HIS), which show anomalous high adsorption. Note that these outliers are consistent with two known factors in carbon surface science:^[5] 1) the higher affinity for planar aromatic or conjugated structures relative to aliphatics, and 2) electrostatic attraction between positively charged solutes and the negatively charged carbon surface (zeta potential -20.4 mV). The weak adsorbers (LEU, ILE, VAL) all have branched aliphatic side chains, which are a poor geometric match to carbon surfaces. Carbon surfaces have a known affinity for planar aromatic structures capable of π - π interactions with the graphene faces on carbon atoms.^[15] The strong adsorbers (ARG, HIS) are basic and carry a positive net charge at physiological pH, as well as having planar sp^2 -hybridized carbon structures in the side chain. The only other basic amino acid is lysine, but it also contains an aliphatic segment that makes it a hybrid of the strong and weak adsorbing subgroups.

The adsorptive depletion of small biomolecular solutes can be reproduced in simple, single-component experiments. Figure 5 shows the interaction of phenol red, tyrosine (an example amino acid), and folic acid (an example vitamin) in simple phosphate-buffered saline (PBS) using UV/visible spectroscopy. Phenol red adsorption is described by the adsorption isotherm in Figure 5a, which also shows the desorption branch determined by successive dilution, and the behavior of functionalized nanotubes with aryl sulfonate groups introduced by diazonium salt chemistry.^[18] The similarity of the adsorption and desorption results indicates reversibility, which is conclusive evidence of physical adsorption. Aryl sulfonation imparts a negative surface charge (reduction in zeta potential from -20.4 to -53.1 mV) and increased hydrophilicity,^[18] and its suppressive effect on adsorption is consistent with a physical adsorption process driven by hydrophobic interactions and opposed by electrostatic repulsion.

Figure 5b shows the equilibrium adsorption isotherm for the amino acid tyrosine in PBS buffer. Here, there is hysteresis between the adsorption and desorption branches that suggests partial irreversibility on the experimental timescale, which is not uncommon in carbon adsorption from solution^[19] due to chemisorption, surface polymerization, or strong multisite physical adsorption or π - π interaction. Figure 5c shows the phenol red adsorption isotherm from Figure 5b (single-component data) superimposed on the same isotherm determined in cell culture medium. The difference shows the effect of the other (>40) components present in the medium, which according to Figure 5c reduces the uptake of phenol red through competition for surface sites. Figure 5d shows equilibrium adsorption isotherms for folic acid in PBS buffer on as-produced and aryl sulfonated SWNTs. Folic acid is taken up rapidly at low doses on the as-produced SWNTs, but to a much lesser extent after aryl sulfonation.

Nanotube adsorption causes profound changes in the composition of the medium, and thus has the potential to influence in vitro cell behavior through an *indirect* mechanism that does not involve physical interaction between nanotubes and target cells. Figure 6a shows that a nanotube dose of only 10 ppm ($10 \mu\text{g mL}^{-1}$) followed by nanotube removal leads to a highly significant inhibitory effect on the viability of HepG2 liver cells. After exposure for 72 h to the depleted medium, the 3-(4,5-dimethylthiazol-2-yl)-5-(3-carboxymethoxyphenyl)-2-(4-sulfophenyl)-2H-tetrazolium inner salt (MTS) assay reports only 50% viability relative to the unaltered medium.

We hypothesized that folate would be one of the most biologically significant of the depleted micronutrients (see Figure 7). Folate deficiency has deleterious effects on DNA metabolism^[20] and this deficiency is exacerbated by deficiency of other vitamins including riboflavin.^[21] In proliferating cells in culture, short-term folate deficiency is known to reduce cell proliferation, induce cell-cycle arrest, trigger apoptosis, and alter expression of micro-RNAs associated with stress responses in primary human lymphocytes as well as lymphoblastoid and hepatocyte cell lines.^[22] To test the specific role of folate depletion in our experiments, we supplemented a variety of the depleted media with external folate and observed reversal of the effect on cell viability (Figure 6b–d). Folate supplementation caused a statistically significant increase in MTS signal after 48 or 72 h in all cases, and accounted for the majority (but not all) of the loss observed by the original multicomponent depletion.

In summary, SWNTs have sufficient surface area to alter the micronutrient content of cell culture medium through adsorption of small-molecule solutes at CNT doses as low as 0.01 mg mL^{-1} . Because physical adsorption is only weakly specific, this is a general phenomenon that influences a broad spectrum of small-molecule solutes including amino acids, vitamins, and indicator/probe dyes. The extent of adsorption is greatest for solutes at low initial concentrations and with a molecular structure favoring adsorption on graphenic carbon—hydrophobicity, planarity/ sp^2 hybridization for π - π interactions, and positive charge (which is opposite to that of most carbon surfaces at neutral pH). Functionalization of the SWNTs with aryl sulfonate groups significantly suppressed adsorption in both cases studied here (phenol red, folic acid), which suggests the dominance of hydrophobic driving forces. The depletion of folate, as well as other essential micro-nutrients at doses of 0.01 – 0.1 mg mL^{-1} , significantly reduced HepG2 cell viability by an indirect mechanism that does not involve physical nanotube–cell interaction. An important implication of this finding is that CNT toxicity, as assessed by commonly used endpoints, such as cell viability, DNA damage, and apoptosis, may be mistakenly attributed to direct toxicity when in fact it is a secondary effect of adsorption of essential micronutrients from cell culture medium. Based on our results, this effect is expected to be much more pronounced for hydrophobic nanotube formulations (as-produced, annealed, or with hydrophobic coatings) than with

tubes functionalized for water solubility. In short-term toxicity assays, these endpoints are potentially reversible by repletion of folate, and cells may adapt to folate depletion by upregulating expression of genes related to folate metabolism.^[24] It is unknown at this time whether folate depletion or altered folate uptake and metabolism would be produced by in vivo exposure to CNTs. However, chronic folate depletion in experimental animals and in humans has been associated with developmental anomalies, particularly neural tube defects, and an increased risk of cardiovascular disease and cancer.^[21]

Experimental Section

Materials and characterization

Purified SWNTs (Carbon Nanotechnologies, Inc.) contained 10% Fe by inductively coupled plasma (ICP) analysis and had a total surface area of $530 \text{ m}^2 \text{ g}^{-1}$ by nitrogen vapor adsorption (Autosorb-1, Quantachrome, Boynton Beach, FL). Iron mobilization from these purified SWNTs in PBS or RPMI medium is very low, as determined by ICP analysis. The SWNTs had zeta potentials (Malvern Instruments Zetasizer Nano-zs, Southborough, MA) of -20.4 (as-produced) and -53.1 mV (after aryl sulfonation). Phenol red and L-tyrosine were purchased from Fisher Scientific Inc. and folic acid (98%) from Sigma. Cell culture media, RPMI medium 1640-11835 (without phenol red) and 1640-11875 (with phenol red), were obtained from Invitrogen Corp.

Nanotube functionalization

To test the effect of hydrophobic surface area on phenol red adsorption, the SWNT sample was functionalized with aryl sulfonate groups to impart hydrophilicity as follows^[18]: SWNTs (1 mg mL^{-1}) were added to a sulfanic acid solution (0.7:480 acid/water weight ratio) and sonicated for 1 h. The solution was placed in a water bath at $70 \text{ }^\circ\text{C}$ and an aqueous NaNO_2 solution (0.28:20 salt/water weight ratio) was added dropwise until the weight ratio of total added salt solution to acid solution reached 1:24. The reaction mixture was stirred for 1 h at $70 \text{ }^\circ\text{C}$ and then quickly cooled. The nanotubes were sedimented by centrifugation at $3900\times g$ in a centrifuge (Centrifugeuses CT422) for 0.5 h, washed five times with deionized water, resedimented, and then dried at $100 \text{ }^\circ\text{C}$.

Adsorption isotherms

Solute solutions (phenol red, tyrosine, or folic acid) were prepared in PBS solution (pH 7.4) at a range of concentrations. SWNTs (as-produced or functionalized) were added and the suspensions sonicated for 30 min (folate for 1 h in low light) followed by 24 h of gentle agitation. Solutions were then transferred to Amicon Ultra-4 centrifugal filter tubes with low-binding Ultracel 5k membranes and centrifuged at $3900\times g$ and $4 \text{ }^\circ\text{C}$ to remove SWNTs. The optical absorbance of the supernatants was measured with a UV/Vis spectrometer (Spectramax M2) at 560 (phenol red), 280 (tyrosine), and 350 nm (folate). For selected samples, the desorption branch of the isotherms was measured by following the same procedure but then diluting to different volumes and incubating for another 24 h prior to centrifugation. To test for competitive adsorption effects, phenol red was added to RPMI 1640-11835 cell culture medium instead of PBS buffer solution and the same procedure was followed.

Amino acid and vitamin profiling

SWNTs were dispersed in RPMI 1640-11875 cell culture medium (without serum) at different doses (from 0.01 to 10 mg mL^{-1}) and sonicated for 30 min. The nanomaterials were then removed by centrifugal ultrafiltration (Amicon Ultra-4 filter tubes). Samples were frozen at $-10 \text{ }^\circ\text{C}$ and spent media analysis was conducted at Sigma-Aldrich (St. Louis, MO), in which amino acids were analyzed by high-performance liquid chromatography

(HPLC; Waters 2695) using UV (Waters 2487) and fluorescence detection (Waters 474) and water-soluble vitamins were analyzed by HPLC (Agilent 1100 CapLC) using tandem mass spectrometric (MS–MS) detection (Thermo Electron LTQ).

HepG2 cell culture in depleted and replenished media

The human hepatoma (HepG2, ATCC HB 8065) cell line was obtained from the American Type Culture Collection. Cell culture medium (minimal essential medium) was obtained from GIBCO-BRL; dialyzed FCS was purchased from Invitrogen and heat inactivated for 30 min at 56 °C. MTS was purchased from Promega. Folate (cell culture tested) was purchased from Sigma–Aldrich. HepG2 cells were incubated at 37 °C in 5% CO₂ for 3 days in folate-free RPMI medium with 5% dialyzed FCS, where they reached a confluency of 80%. After trypsination with 1% trypsin/ethylenediaminetetraacetic acid (EDTA), the cells were split equally into two flasks and cultured with fresh folate-free medium for an additional 3 days. The cells were trypsinized with 1% trypsin/EDTA, seeded into 96-well plates at 25 000 cells per well, and incubated overnight at 37 °C with fresh medium. After 24 h, the medium was replaced with the following media containing 5% dialyzed FCS: folate-free RPMI; folate-free RPMI supplemented with 1 mg L⁻¹ folate; 10 µg mL⁻¹ CNT-incubated RPMI; 10 µg mL⁻¹ CNT-incubated RPMI supplemented with 1 mg L⁻¹ folate; 1 mg mL⁻¹ CNT-incubated RPMI; 1 mg mL⁻¹ CNT-incubated RPMI supplemented with 1 mg L⁻¹ folate; and RPMI containing folate as a control.

Viability, which is determined by the measurement of the quantity of formazan product by MTT reduction, was measured after 24, 48, and 72 h by MTS assay at a wavelength of 490 nm using a Spectramax M2 microtiter plate reader (Molecular Devices). All assays were conducted in quadruplicate and repeated at least three times.

Acknowledgments

Although this work was supported in part by the NIEHS and EPA, the results do not necessarily represent the views of either agency.

References

1. a) Worle-Knirsch JM, Pulskamp K, Krug HF. *Nano Lett.* 2006; 6:1261–1268. [PubMed: 16771591] (b) Smart SK, Cassady AI, Lu GQ, Martin DJ. *Carbon.* 2006; 44:1034–1047. (c) Casey A, Davoren M, Herzog E, Lyng FM, Byrne HJ, Chambers G. *Carbon.* 2007; 45:34–40. (d) Casey A, Davoren M, Herzog E, Lyng FM, Byrne HJ, Chambers G. *Carbon.* 2007; 45:1425–1432.
2. a) Smart SK, Cassady AI, Lu GQ, Martin DJ. *Carbon.* 2006; 44:1034–1047. (b) Sager TM, Porter DW, Robinson VA, Lindsley WG, Schwegler-Berry DE, Castranova V. *Nanotoxicology.* 2007; 1:1–12.
3. a) Worle-Knirsch JM, Pulskamp K, Krug HF. *Nano Lett.* 2006; 6:1261–1268. [PubMed: 16771591] (b) Monteiro-Riviere NA, Inman AO. *Carbon.* 2006; 44:1070–1078. (c) Casey A, Davoren M, Herzog E, Lyng FM, Byrne HJ, Chambers G. *Carbon.* 2007; 45:34–40. (d) Casey A, Davoren M, Herzog E, Lyng FM, Byrne HJ, Chambers G. *Carbon.* 2007; 45:1425–1432. (e) Zhang LW, Zeng L, Barron AR, Monteiro-Riviere NA. *Int J Toxicol.* 2007; 26:103–113. [PubMed: 17454250] (f) Isobe H, Tanaka T, Maeda R, Noiri E, Solin N, Yudasaka M, Iijima S, Nakamura E. *Angew Chem.* 2006; 118:6828–6832. *Angew Chem Int Ed.* 2006; 45:6676–6680.
4. a) Worle-Knirsch JM, Pulskamp K, Krug HF. *Nano Lett.* 2006; 6:1261–1268. [PubMed: 16771591] (b) Monteiro-Riviere NA, Inman AO. *Carbon.* 2006; 44:1070–1078. (c) Casey A, Davoren M, Herzog E, Lyng FM, Byrne HJ, Chambers G. *Carbon.* 2007; 45:1425–1432.
5. a) Radovic, L.; Moreno-Castilla, C.; Rivera-Utrilla, J. *Chemistry and Physics of Carbon.* Radovic, L., editor. Vol. 27. Marcel Dekker; New York: 2000. p. 290–312. (b) Liu Z, Sun X, Nakayama-Ratchford N, Dai H. *ACS Nano.* 2007; 1:50–56. [PubMed: 19203129]
6. Worle-Knirsch JM, Pulskamp K, Krug HF. *Nano Lett.* 2006; 6:1261–1268. [PubMed: 16771591]

7. a) Casey A, Davoren M, Herzog E, Lyng FM, Byrne HJ, Chambers G. Carbon. 2007; 45:34–40.(b) Casey A, Davoren M, Herzog E, Lyng FM, Byrne HJ, Chambers G. Carbon. 2007; 45:1425–1432.
8. Monteiro-Riviere NA, Inman AO. Carbon. 2006; 44:1070–1078.
9. Zhang LW, Zeng L, Barron AR, Monteiro-Riviere NA. Int J Toxicol. 2007; 26:103–113. [PubMed: 17454250]
10. a) Zheng M, Jagota A, Strano MS, Santos AP, Barone P, Chou SG, Diner BA, Dresselhaus MS, McLean RS, Onoa GB, Samsonidze GG, Semke ED, Usrey M, Walls DJ. Science. 2003; 302:1545–1548. [PubMed: 14645843] (b) Lu G, Maragakis P, Kaxiras E. Nano Lett. 2005; 5:897–900. [PubMed: 15884890] (c) Singh R, Pantarotto D, McCarthy D, Chaloin O, Hoebeke J, Partidos CD, Briand JP, Prato M, Bianco A, Kostarelos K. J Am Chem Soc. 2005; 127:4388–4396. [PubMed: 15783221] (d) Salvador-Morales C, Townsend P, Flahaut E, Vénien-Bryan C, Vlandas A, Green MLH, Sim RB. Carbon. 2007; 45:607–617.(e) Song L, Meng J, Zhong J, Liu L, Dou X, Liu D, Zhao X, Luo S, Zhang Z, Xiang Y, Xu H, Zhou W, Wu Z, Xie S. Colloids Surf B. 2006; 49:66–70.(f) Meng J, Song L, Xu H, Kong H, Wang C, Guo X, Xie S. Nanomed Nanotechnol Biol Med. 2005; 1:136–142.(g) MacDonald AR, Laurenzi FB, Viswanathan G, Ajayan MP, Stegemann PJ. J Biomed Mater Res A. 2005; 74:489–496. [PubMed: 15973695]
11. Roman T, Dino WA, Nakanishi H, Kasai H. Eur Phys J D. 2006; 38:117–120.
12. Liu X, Gurel V, Morris D, Murray D, Zhitkovich A, Kane AB, Hurt RH. Adv Mater. 2007; 19:2790–2796.
13. Casey A, Davoren M, Herzog E, Lyng FM, Byrne HJ, Chambers G. Carbon. 2007; 45:34–40.
14. Guo L, Morris DG, Liu X, Vaslet C, Hurt RH, Kane AB. Chem Mater. 2007; 19:3472–3478.
15. a) Radovic, L.; Moreno-Castilla, C.; Rivera-Utrilla, J. Chemistry and Physics of Carbon. Radovic, L., editor. Vol. 27. Marcel Dekker; New York: 2000. p. 290-312.b) Hurt RH, Krammer G, Crafwford G, Jian K, Rulison C. Chem Mater. 2002; 14:4558–4565.(c) Chen RJ, Zhang Y, Wang D, Dai H. J Am Chem Soc. 2001; 123:3838–3839. [PubMed: 11457124]
16. Black DS, Mould RD. Anal Biochem. 1991; 193:72–82. [PubMed: 2042744]
17. Rekker, RF. The Hydrophobic Fragmental Constant. Elsevier; Amsterdam: 1977.
18. Yan A, Xiao X, Kulaots I, Sheldon B, Hurt RH. Carbon. 2006; 44:3116–3120.
19. a) Radovic, L.; Moreno-Castilla, C.; Rivera-Utrilla, J. Chemistry and Physics of Carbon. Radovic, L., editor. Vol. 27. Marcel Dekker; New York: 2000. p. 290-312.b) Chen RJ, Zhang Y, Wang D, Dai H. J Am Chem Soc. 2001; 123:3838–3839. [PubMed: 11457124]
20. Friso S, Choi S-W. Curr Drug Metab. 2005; 6:37–46. [PubMed: 15720206]
21. Stover PJ. Nutr Rev. 2004; 62:53–512.
22. a) Courtemanche C, Elson-Schwab I, Mashiyama ST, Kerry N, Ames BN. J Immunol. 2004; 173:3186–3192. [PubMed: 15322179] (b) Lin JL, Chen CJ, Tsai WC, Yen JH, Liu HW. Br J Nutr. 2006; 95:820–898.(c) Marsit CJ, Eddy K, Kelsey KT. Cancer Res. 2006; 66:10843–10848. [PubMed: 17108120]
23. a) Friso S, Choi SW. Curr Drug Metab. 2005; 6:37–46. [PubMed: 15720206] (b) Stover PJ. Nutr Rev. 2004; 62:53–512.
24. Hayashi I, Sohn KJ, Stempak JM, Croyford R, Kim YI. J Nutr. 2007; 137:607–613. [PubMed: 17311948]

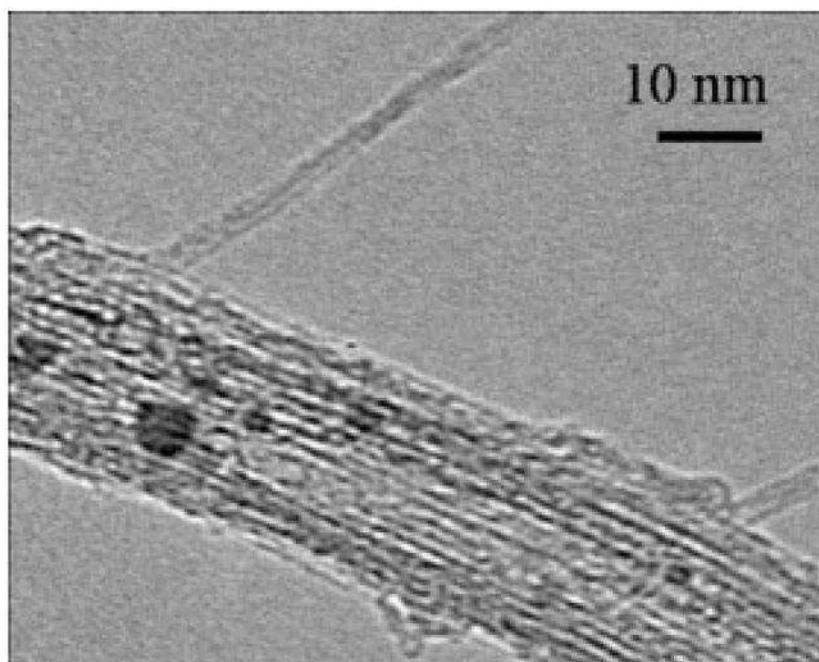


Figure 1. High-resolution transmission electron microscopy (TEM) image of the typical morphology of the SWNT sample used in this study. Most tubes exist as ordered bundles, and both amorphous carbon and iron-containing catalyst particles are seen as minority features in this purified sample. The release and redox activity of the iron residues have been characterized previously,^[14] and for this purified sample are low in cell culture medium.

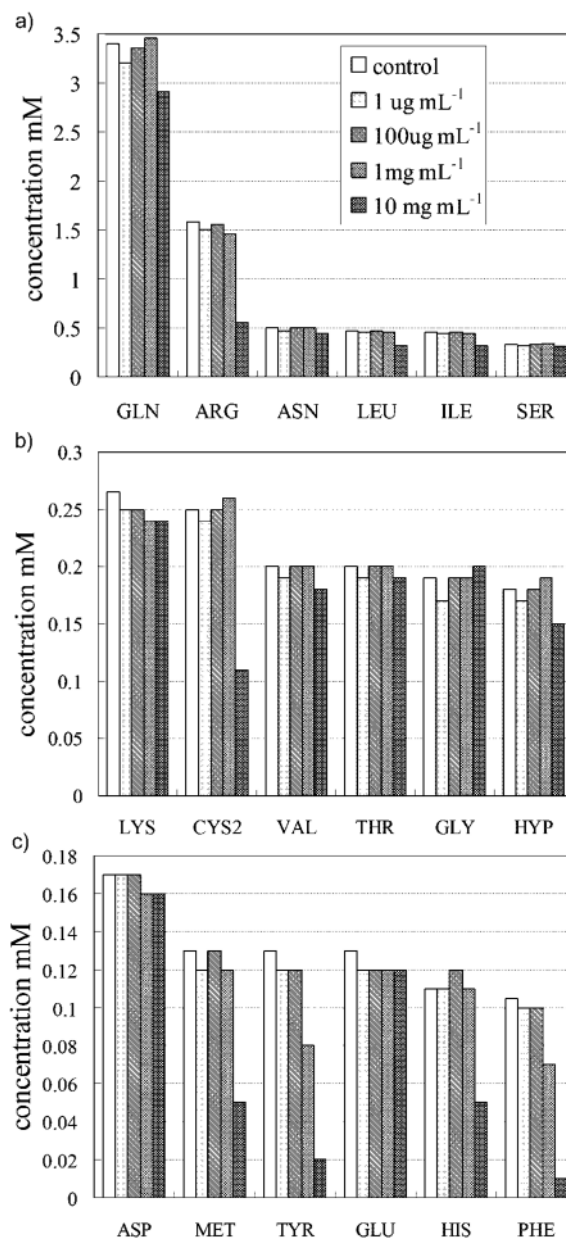


Figure 2. Amino acid profiling in RPMI 1640-11875 cell culture medium as a function of SWNT dose. The amino acids are placed into three groups according to their starting concentration in cell culture medium from highest (a) to lowest (c). A typical standard deviation in this assay is 0.01 mM.

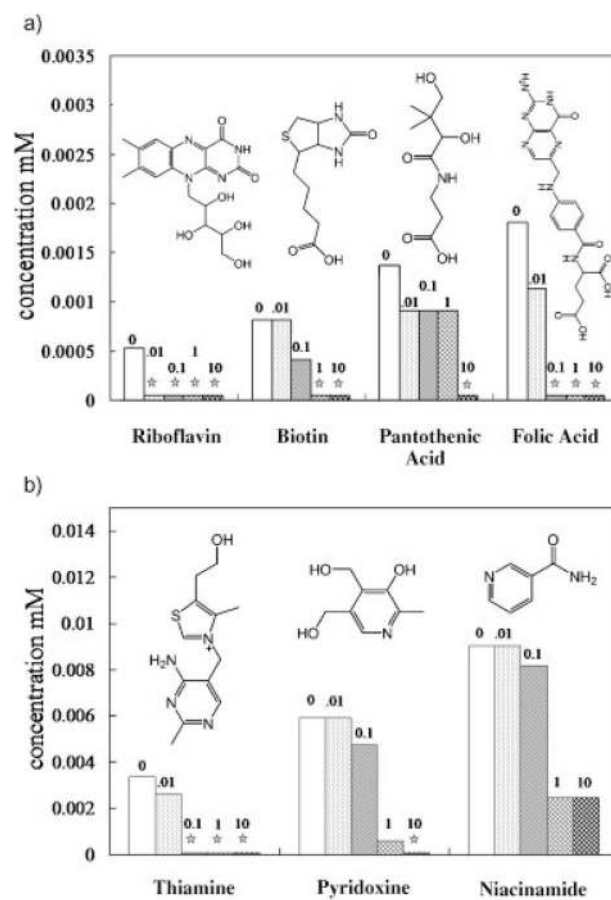


Figure 3. Vitamin profiling of RPMI 1640-11875 cell culture medium as a function of SWNT dose. The numbers above the bars show the CNT dose in mg mL^{-1} . Typical standard deviations for this assay are 0.0002 mM in the lower concentration range (a) and 0.001 mM in the higher concentration range (b). Asterisks indicate concentrations below the detection limit.

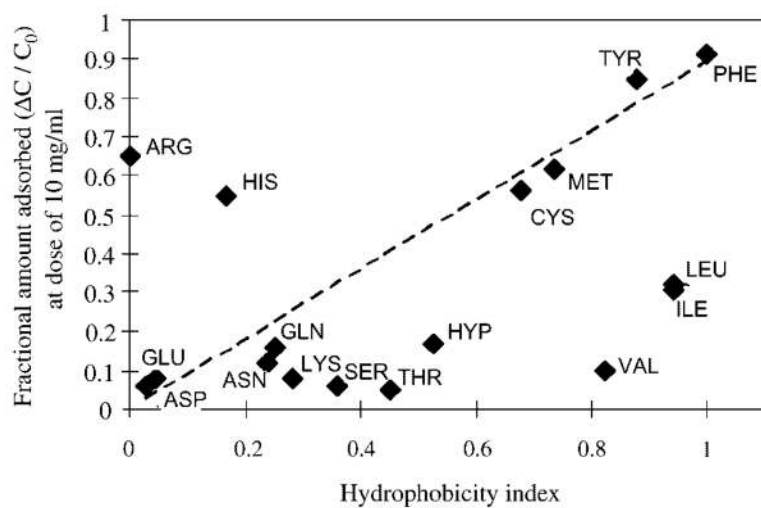


Figure 4. Relative affinity of SWNTs for various amino acids from Figure 2 versus the side-chain hydrophobicity index of Black and Mould. ^[16]

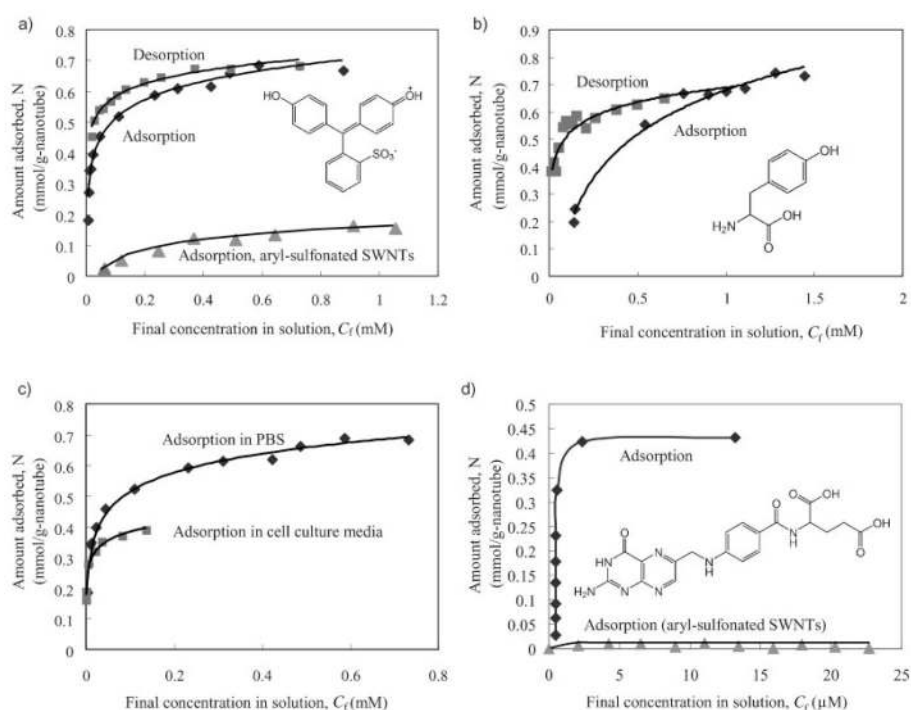
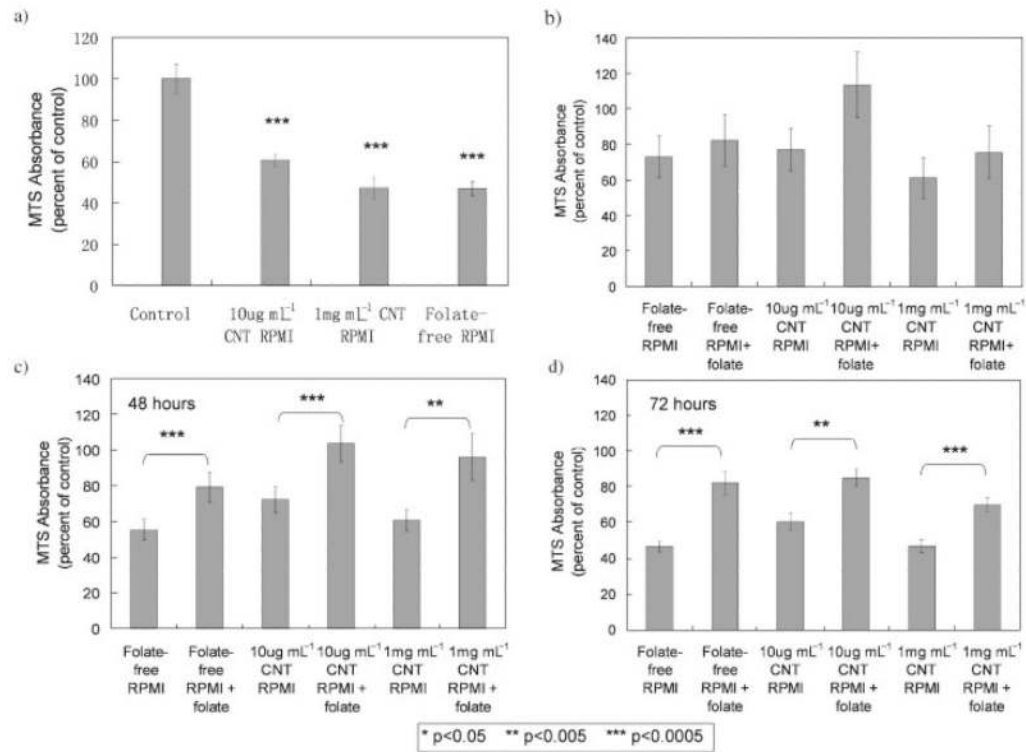


Figure 5. Results of single-component adsorption experiments on SWNTs with selected solutes. a) Fundamental adsorption/desorption isotherms for phenol red on as-produced SWNTs (top curves) and SWNTs functionalized by aryl sulfonation (bottom curve). b) Adsorption/desorption isotherms for the aromatic amino acid tyrosine in PBS. c) Comparison of phenol red isotherms as a single component (top curve, in PBS) and in the presence of other organic solutes (bottom curve, in cell culture medium). The difference reflects competition for adsorption sites among the >40 medium components. d) Adsorption isotherms for folic acid on as-produced and sulfonated SWNTs in PBS buffer.

**Figure 6.**

Viability of HepG2 cells incubated in various RPMI media using the MTS assay. Hep2 cells were incubated for 7 days in folate-free RPMI with 5% dialyzed fetal calf serum (FCS). Cells were seeded into 96-well plates at 25 000 cells per well containing fresh medium. After 24 h, the medium was replaced with the following media containing 5% dialyzed FCS: folate-free RPMI; folate-free RPMI supplemented with 1 mg L⁻¹ folate; 10 μg mL⁻¹ CNT-depleted RPMI; 10 μg mL⁻¹ CNT-depleted RPMI supplemented with 1 mg L⁻¹ folate; 1 mg mL⁻¹ CNT-depleted RPMI; 1 mg mL⁻¹ CNT-depleted RPMI supplemented with 1 mg L⁻¹ folate; and RPMI containing folate as a control. a) Effect of CNT dose on cell viability after 72 h with folate-free medium as a positive control. The *p* values give statistical significance relative to undepleted RPMI as a negative control. b–d) Detailed time-dependent behavior of the effects of folate repletion; cell viability after b) 24, c) 48, and d) 72 h. The *p* values compare the depleted (or folate-free) medium with its respective folate-replenished medium and thus show the statistical significance of folate replenishment.

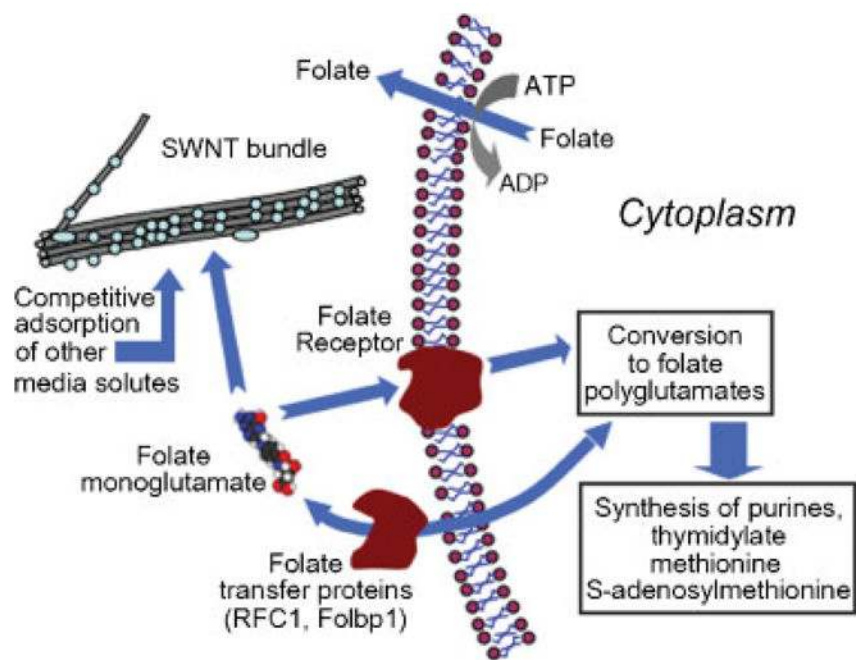


Figure 7. Regulation of transport of folate monoglutamate (folic acid) and intracellular folate metabolism^[21] adapted to show competitive adsorption on CNTs. Folate is an essential water-soluble B vitamin involved in one-carbon transfer reactions and required for nucleotide synthesis and for conversion of homocysteine to methionine.^[23] Folate enters cells by the reversible action of transfer proteins and by unidirectional membrane-bound folate receptors, where it accumulates only after conversion to folate polyglutamates.^[21] Cell-culture and animal models have shown that folate deficiency inhibits DNA synthesis, induces DNA mutations and strand breaks, impairs DNA repair, and alters DNA methylation patterns.^[20]